

# Electrical characterization of conducting polypyrrole by THz time-domain spectroscopy

Tae-In Jeon<sup>a)</sup> and D. Grischkowsky<sup>b)</sup>

*School of Electrical and Computer Engineering and Center for Laser and Photonics Research, Oklahoma State University, Stillwater, Oklahoma 74078*

A. K. Mukherjee and Reghu Menon

*Department of Physics, Indian Institute of Science, Bangalore, India*

(Received 31 July 2000; accepted for publication 24 August 2000)

Using an optoelectronic THz beam system for THz time-domain spectroscopy (THz TDS), we have measured the absorption and index of refraction of a conducting polypyrrole film from low frequencies to 2.5 THz. From these measurements, the dc conductivity of 215/( $\Omega$  cm) and the complex conductance were obtained over this frequency range. All of the results were well fit by Drude theory, which gives a carrier scattering time of only 12.6 fs, less than 1/10 that of the semiconductors, thereby illustrating the disorder and low mobility of the polymer. © 2000 American Institute of Physics. [S0003-6951(00)05242-6]

It has been a problem of long-standing and sustained interest to electrically characterize and understand the electrical transport properties of the conducting polymers,<sup>1</sup> and in particular, conducting polypyrrole.<sup>2-4</sup> THz time-domain spectroscopy (THz TDS) appears to be the ideal tool to characterize the carrier dynamics in conducting polymers, as demonstrated by the previous THz-TDS characterizations of semiconductors.<sup>5-10</sup> In contrast to metals and semiconductors, it is not possible to electrically characterize conducting polymers by simple electrical measurements using mechanical contacts, e.g., Hall-effect measurements. For such characterization Ohmic contacts would have to be fabricated on the polymer itself. The direct measurement of the mobility and relaxation time by contactless THz TDS would be highly desirable. Moreover, the uncertainties involved in using the Kramers-Kronig analysis in the usual far-infrared spectroscopy can be avoided with THz TDS.

In the simple Drude theory picture of conduction the key parameters describing the dynamics of free carriers in a material are the plasma frequency  $\omega_p$  and the carrier damping rate  $\Gamma=1/\tau$ , where  $\tau$  is the carrier collision time. Because  $\omega_p$  and  $\Gamma$  characteristically have THz values, measurements spanning the values of these parameters must be performed in the THz frequency range.<sup>5-10</sup> The experiments described in this letter present such THz-TDS measurements on a film of conducting polypyrrole.<sup>2-4</sup> The free-standing 10- $\mu$ m-thick films of Ppy-Pf6 with a room-temperature conductivity of 215/( $\Omega$  cm) are prepared electrochemically at  $-40^\circ\text{C}$ . Our results show the absorption and index of refraction of conducting polypyrrole from low frequencies to beyond 2.5 THz. The fact that the measured frequency-dependent absorption and index of refraction are mostly due to the free carriers, allows the complex conductivity to be determined from the measurements over the full frequency range. The results are well fit by the Drude theory.

The THz-TDS characterizations were performed by measuring freely propagating, THz electromagnetic pulses transmitted through the thin polymer film under investigation. These transmitted pulses were then compared to the measured THz pulses with no sample in place. Analysis of the respective numerical Fourier transforms determines the frequency-dependent absorption and index of refraction.

The measured 0.38 ps reference pulse with no sample in place is shown in Fig. 1(a), which is the average of seven individual measurements to thereby increase the signal-to-noise ratio (S/N). With the sample placed in the THz beam the transmitted pulse shown in Fig. 1(b) was obtained, where the measured amplitude has dropped by approximately 100 and the pulse width has increased to 0.44 ps. This wave form is the average of 27 individual measurements. The resulting noise for the transmitted pulse is 0.05 pA (rms), yielding a S/N=400. In terms of the input pulse the amplitude dynamic range (S/N) of this time-domain experiment is 40 000. The normalized amplitude spectrum of the input reference pulse is shown as the top curve in Fig. 1(c) together with the spectrum of the transmitted output pulse shown as the lower curve (multiplied 50 $\times$ ) on the same relative scale. The amplitude S/N=100 for the output spectrum gives a total S/N=5000 when compared to the input spectrum. The very large frequency-dependent absorption of the sample is clearly evident.

The frequency-dependent complex dielectric constant  $\epsilon$  of the sample is equal to the square of the complex index of refraction  $n=n_r+in_i$ . The imaginary index  $n_i$  is determined by measuring the power absorption coefficient  $\alpha=n_i4\pi/\lambda_0$ . For our experimental situation with a highly absorbing sample, the reflection of the THz pulse from the output face of the sample may be neglected. For this situation, the complex ratio of the output amplitude spectrum of the transmitted THz pulse to the input spectrum of the reference pulse simplifies to the following:

$$E_0(\omega)/E_{\text{Ref}}(\omega)=t_{12}t_{21}\exp i(k-k_0)L\exp(-\alpha L/2), \quad (1)$$

where  $t_{12}$  is the Fresnel transmission coefficient from air into

<sup>a)</sup>Permanent address: Department of Electrical Engineering, Korea Maritime University, Pusan, Korea.

<sup>b)</sup>Electronic mail: grischd@master.ceat.okstate.edu

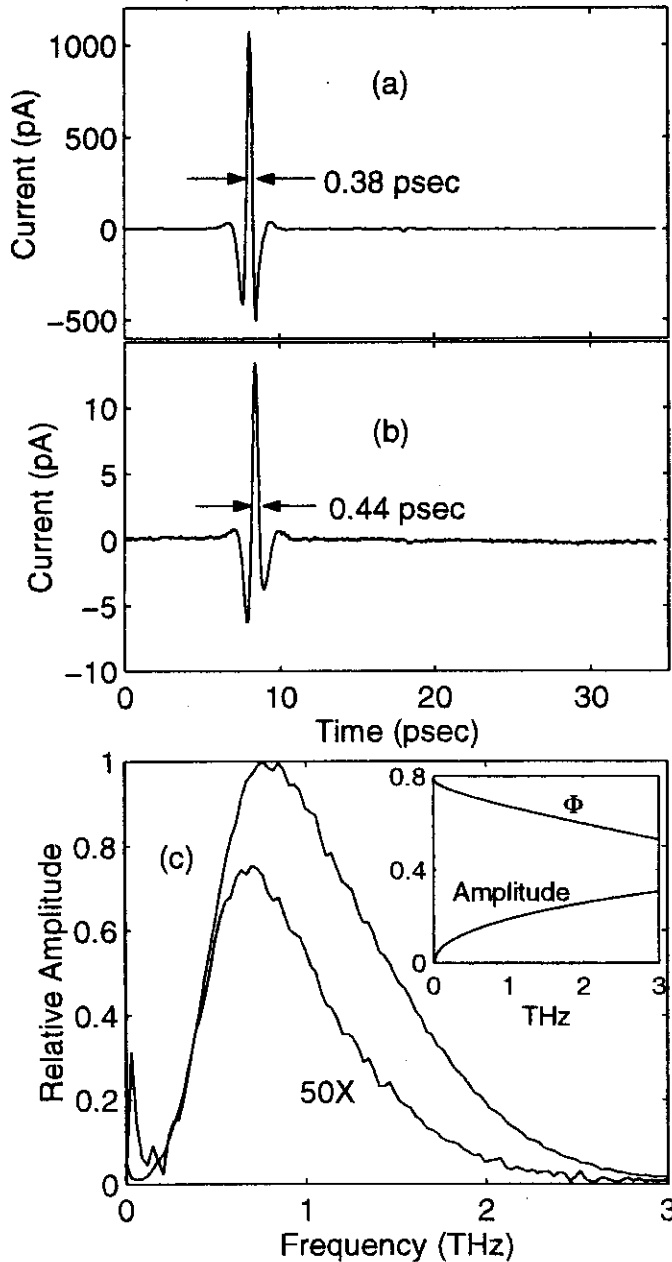


FIG. 1. (a) Measured reference input THz pulse. (b) Measured output THz pulse transmitted through sample. (c) Amplitude spectra of input pulse and transmitted pulse (spectrum multiplied by 50X); inset, calculated phase  $\Phi$  (upper curve) in radians of  $t_{12}t_{21}$ , together with the amplitude  $|t_{12}t_{21}|$ .

the sample of length  $L$  and  $t_{21}$  is the transmission coefficient from the sample into air at the output; the propagation vectors are  $k = 2\pi n_r/\lambda$ , and  $k_0 = 2\pi/\lambda$ ;  $\alpha$  is the power absorption coefficient.  $t_{12}t_{21}$  is complex and strongly frequency dependent, due to the strong frequency dependence of the complex index  $n$  and the exceptionally high absorption; with the index of air set equal to unity,  $t_{12}t_{21}$  is given by

$$t_{12}t_{21} = 4n/(1+n)^2 = |t_{12}t_{21}| \exp i\Phi. \quad (2)$$

For the data analysis,  $|t_{12}t_{21}|$  is used for the determination of  $\alpha$ , while the frequency-dependent phase shift  $\Phi$  must be used in the determination of  $n_r$ . It is clear that an iterative procedure must be employed, because  $|t_{12}t_{21}|$  is determined by  $n$  and  $\Phi$  and vice versa. In order to obtain the absorption of the sample shown in Fig. 2(a), the output amplitude spectrum shown in Fig. 1(c) must be divided by the  $|t_{12}t_{21}|$  curve, and

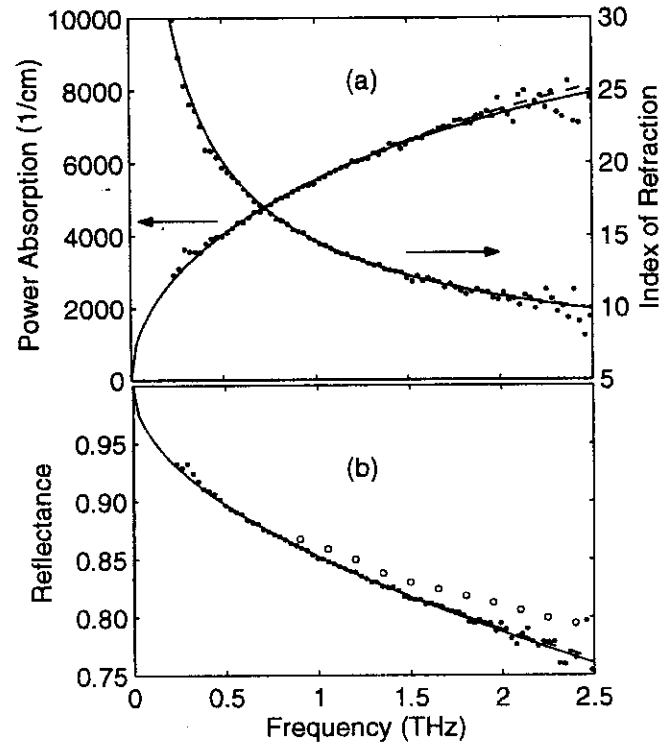


FIG. 2. Drude theory (solid lines our parameters, dashed lines parameters of Ref. 4) and measurements (solid dots) for the conducting polypyrrole sample. (a) Power absorption coefficient (left axis, increasing curve) and the index of refraction  $n_r$  (right axis, decreasing curve). (b) Reflectance  $R$ . Open circles are measurements from Ref. 4.

in order to determine the index of refraction  $n_r$ , the additional phase term  $\Phi$  must be subtracted from the phase difference between the frequency components of the reference and transmitted pulse. For comparison with the previous work,<sup>2-4</sup> we also plot the power reflectance  $R$  obtained from our data as the dots in Fig. 2(b).

Our THz-TDS measurements of the exceptionally high absorption of the conducting polymer sample are shown in Fig. 2(a). Even though the free-standing film thickness  $L$  was only 10  $\mu\text{m}$ , due to the strong absorption and decreasing spectral amplitude, the measurements were limited to 2.5 THz. Compared to the measured absorptions for the conducting polymers, the absorption of the undoped host polymer is negligible. The measured strong frequency dependence of the index of refraction decreases monotonically by a factor of 3 from low to high frequencies. The reflectance  $R = r_{12}r_{12}^*$  obtained from the measured  $n = n_r + in_i$ , as determined from Fig. 2(a) where  $r_{12} = (1-n)/(1+n)$ , is presented in Fig. 2(b). The solid dots are our measurements and the open circles are the reflectance measurements of Ref. 4.

The conducting polymer's dielectric response is described by the general relationship,

$$\epsilon = \epsilon_{\text{Poly}} + i\sigma/(\omega\epsilon_0) = (n_r + in_i)^2, \quad (3)$$

where  $\epsilon_{\text{Poly}}$  is the dielectric constant of the undoped polymer,  $\sigma$  is the complex conductivity, and  $\epsilon_0$  is the free-space permittivity. Given that our measured index data are  $n_r$  and that the absorption data determine  $n_i$ , and given  $\epsilon_{\text{Poly}}$ , the real part  $\sigma_r$  and the imaginary part  $\sigma_i$  of the conductivity can be obtained from Eq. (3). A causal conductivity requires a positive monotonically increasing  $\sigma_i$ ; for our case, this require-

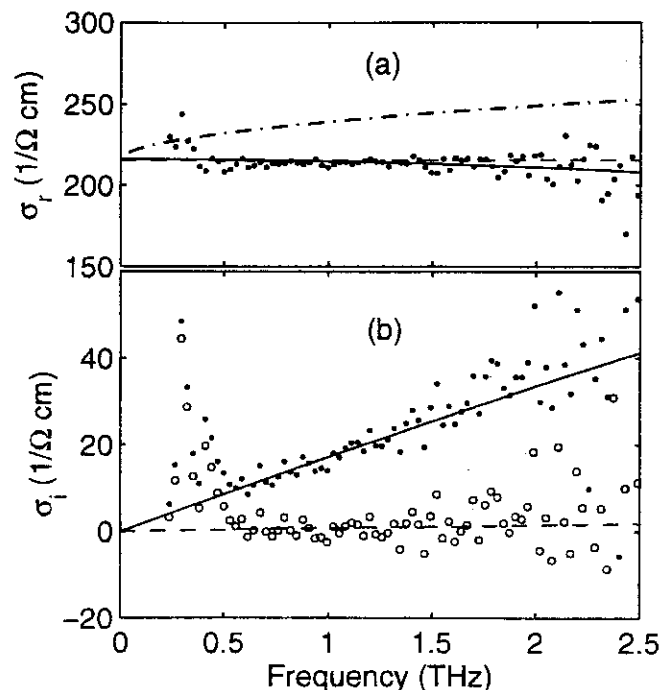


FIG. 3. Complex conductivity obtained from the measurements. Solid lines are Drude theory with our parameters. Dashed lines are Drude theory with the parameters of Ref. 4. (a) Real part of the conductivity. Upper dot-dash curve is from the localized-modified Drude model (see Ref. 4). (b) The imaginary part of the conductivity; upper curve with  $\epsilon_{\text{poly}}=70$  (solid dots), and the lower curve with  $\epsilon_{\text{poly}}=40$  (open circles).

ment indicates that  $\epsilon_{\text{poly}} > 35$ . Here,  $\epsilon_{\text{poly}}=70$  was used in order to achieve a  $\sigma_i$  [shown as the upper curve with the dots in Fig. 3(b)] which linearly increases from zero and remains significantly smaller than  $\sigma_r$  up to 2.5 THz. As shown in Fig. 3(a), the corresponding  $\sigma_r$  slightly decreases with increasing frequency, contrary to the predictions of an increase with frequency due to a weak localization.<sup>4</sup> The extrapolated zero-frequency value gives the high dc conductivity of 215/ $\Omega$  cm.

As can be seen in Fig. 2(a), from low frequencies up to 2.5 THz the absorption measurements (dots) are well described by the absorption calculated from  $n_i$  using Eq. (1),  $\epsilon_{\text{poly}}=70$ , and  $\sigma$  of the Drude model, which treats the free carriers in a solid as classical point charges subject to random collisions and yields the complex conductivity

$$\sigma = i\epsilon_0\omega_p^2/(\omega + i\Gamma). \quad (4)$$

The Drude theory fit to the measured index of refraction is quite good over the entire frequency range, as is the fit to the reflectance data of Fig. 2(b). Considering the simplicity of the two parameter Drude model, this excellent agreement is noteworthy; the Drude theory parameters are  $\omega_p/(2\pi)=70$  THz and  $\Gamma/(2\pi)=12.6$  THz, corresponding to  $\tau=12.6$  fs. This very short time between collisions is approximately 1/10 of that for the doped semiconductors Si and GaAs with

similar conductivity and illustrates the disorder and low mobility  $\mu$  of the polymer. As used in Drude theory  $\omega_p^2 = Ne^2/(\epsilon_0 m^*)$ , where  $N$  is the carrier density,  $e$  is the charge on the electron, and  $m^*$  is the effective mass of the electron;  $\Gamma = e/(m^* \mu)$ . The effective mass has been calculated to be  $m^* = 1.7 m_e$ ,<sup>4</sup> where  $m_e$  is the free-electron mass. Using this value, we calculate the high carrier density  $N = 1 \times 10^{20}/\text{cm}^3$ , and the very low mobility  $\mu = 13 \text{ cm}^2/\text{V s}$ .

The above values for the Drude parameters can be directly compared with those of previous work based on broadband reflectivity measurements,<sup>4</sup> for conducting polypyrrole in the metallic regime, for which  $\omega_p/(2\pi)=438$  THz and  $\Gamma/(2\pi)=288$  THz, corresponding to the extraordinarily short collision time of  $\tau=0.55$  fs. We have tried to fit our data with these parameters. An excellent fit, shown as the dashed lines in Figs. 2(a) and 2(b) and Figs. 3(a) and 3(b) was obtained with the plasma frequency slightly reduced to  $\omega_p/(2\pi)=334$  THz (to fit our extrapolated dc conductivity) and  $\Gamma/(2\pi)=288$  THz, together with  $\epsilon_{\text{poly}}=40$ . These parameters give the very high carrier density of  $N=2.3 \times 10^{21}/\text{cm}^3$ . It is important to note that  $\sigma_i$  extracted from the measurements depends strongly on  $\epsilon_{\text{poly}}$ , thereby explaining the two sets of results in Fig. 3(b). The fit is so good that the solid and dashed curves cannot be distinguished for the index, and only can be distinguished at the highest frequencies for the absorption, reflectance, and real part of the conductivity. Clearly, the discrepancy between these two sets of parameters cannot be resolved by our measurements, where the obtained real part of the conductivity is almost constant from low frequencies to 2.5 THz. However, as shown in Fig. 3(a), the localized-modified Drude model<sup>4</sup> does not appear to describe our measurements of  $\sigma_r$ . Here, we have confidence in our results, which were obtained directly and without the added complication of a Kramers-Kronig analysis.

The Oklahoma State part of this work was partially supported by the National Science Foundation and the Army Research Office.

<sup>1</sup>R. Menon, C. O. Yoon, D. Moses, and A. J. Heeger, in *Handbook of Conducting Polymers*, edited by T. A. Skotheim, R. L. Elsenbaumer, and J. R. Reynolds (Marcel Dekker, New York, 1998).

<sup>2</sup>C. O. Yoon, R. Menon, D. Moses, and A. J. Heeger, *Phys. Rev. B* **49**, 10851 (1994).

<sup>3</sup>R. Menon, C. O. Yoon, D. Moses, and A. J. Heeger, *Synth. Met.* **64**, 53 (1994).

<sup>4</sup>K. Lee, R. Menon, C. O. Yoon, and A. J. Heeger, *Phys. Rev. B* **52**, 4779 (1995).

<sup>5</sup>D. Grischkowsky, S. Keiding, M. van Exter, and Ch. Fattinger, *J. Opt. Soc. Am. B* **7**, 2006 (1990).

<sup>6</sup>M. van Exter and D. Grischkowsky, *Appl. Phys. Lett.* **56**, 1694 (1990); *Phys. Rev. B* **41**, 12140 (1990).

<sup>7</sup>N. Katzenellenbogen and D. Grischkowsky, *Appl. Phys. Lett.* **61**, 840 (1992).

<sup>8</sup>T.-I. Jeon and D. Grischkowsky, *Phys. Rev. Lett.* **78**, 1106 (1997).

<sup>9</sup>T.-I. Jeon and D. Grischkowsky, *Appl. Phys. Lett.* **72**, 2259 (1998).

<sup>10</sup>T.-I. Jeon and D. Grischkowsky, *Appl. Phys. Lett.* **72**, 3032 (1998).